Chinese Chemical Letters 31 (2020) 1931–1935

Contents lists available at ScienceDirect

Chinese Chemical Letters

journal homepage: www.elsevier.com/locate/cclet

Communication

Synthesis and self-assembly of poly(ethylene glycol)-*block*-poly(*N*-3-(methylthio)propyl glycine) and their oxidation-sensitive polymersomes

Yangwei Deng[a,b], Hui Chen[a], Xinfeng Tao[a,e], Sylvain Trépout[d], Jun Ling[b,*], Min-Hui Li[a,c,**]

[a] *Chimie ParisTech, PSL University Paris, CNRS, Institut de Recherche de Chimie Paris, Paris 75005, France*
[b] *MOE Key Laboratory of Macromolecular Synthesis and Functionalization, Department of Polymer Science and Engineering, Zhejiang University, Hangzhou 310027, China*
[c] *Beijing Advanced Innovation Center for Soft Matter Science and Engineering, Beijing University of Chemical Technology, Beijing 100029, China*
[d] *Institut Curie, Inserm US43, University Paris Saclay, Orsay Cedex 91405, France*
[e] *Shanghai Key Laboratory of Advanced Polymeric Materials, School of Materials Science and Engineering, East China University of Science and Technology, Shanghai 200237, China*

ARTICLE INFO

Article history:
Received 23 November 2019
Received in revised form 16 December 2019
Accepted 17 December 2019
Available online 18 December 2019

Keywords:
Polypeptoid
Self-assembly
Polymersome
Oxidation-responsive
Glucose oxidase

ABSTRACT

Amphiphilic block copolymers poly(ethylene glycol)-*block*-poly(*N*-3-(methylthio)propyl glycine) (PEG-*b*-PMeSPG) were synthesized *via* ring-opening polymerization of *N*-3-(methylthio)propyl glycine *N*-thiocarboxyanhydride (MeSPG-NTA) initiated by amino-terminated PEG. The self-assemblies of three PEG-*b*-PMeSPG copolymers with different PMeSPG block lengths were first prepared by nano-precipitation method using THF and DMF, respectively, as the organic solvent, and their morphologies were studied by Cryo-EM and DLS. To prepare polymersomes loaded with glucose oxidase (GOx), double emulsion method followed by extrusion treatment was employed. The oxidation-responsive disruption of polymersomes was achieved upon the introduction of glucose because of the oxidants generated *in-situ* by GOx/glucose.

Polypeptoids are polymers composed of *N*-substituted amino acids [1–3]. With polyglycine backbones which are similar to polypeptides, polypeptoids exhibit excellent biocompatibility and biodegradability [4–6]. Meanwhile, the side chains substituting the hydrogen on the nitrogen atom of amides avoid the formation of intra- and intermolecular hydrogen bonds. Consequently, polypeptoids exhibit much better solubility in common organic solvents than polypeptides. Various *N*-substituting side groups can be utilized to tailor the physicochemical and biological properties of the polypeptoids, which endows polypeptoids with various functions [7–10].

The self-assembly of amphiphilic block copolymers in water can form a variety of nanostructures, including micelles, vesicles and lamellae [11]. Recently, self-assembled nanostructures based on polypeptoids have received increasing interests [8,12–18]. For example, Zhang *et al.* designed a series of ABC block copolypeptoids composed of hydrophilic, hydrophobic and thermo-responsive segments, which formed spherical and short cylindrical micelles in aqueous solutions at low temperature ($T < T_c$), and underwent reversible sol-to-gel transition at high temperature ($T \geq T_c$). They applied this thermo-sensitive transition to chondrogenesis experiments of cells and encapsulation of enzymes [15]. The same group also reported highly efficient gene-transfection polyplexes by introducing cationic side groups [16] and redox-responsive micelles [17] by adding disulfide linkages in the *N*-substituents. Our group reported micelles and polymersomes with aggregation-induced emission (AIE) made from the amphiphilic diblock copolypeptoids of polysarcosine (PSar) and tetraphenylethylene (TPE)-modified poly(*N*-allyl glycine) [18]. These AIE nanoparticles showed strong fluorescence emission and non-cytotoxicity, which suggested promising applications in biomedical fields.

Among the various nanostructures formed by amphiphilic block copolymers, polymer vesicles, also called as polymersomes, which can be disrupted upon external stimuli, and then release encapsulated substances, are especially interesting and have been developed as attractive nanocarriers for drug delivery applications [19–23]. Here we are interested in the polypeptoid vesicles

* Corresponding author.
** Corresponding author at: Chimie ParisTech, PSL University Paris, CNRS, Institut de Recherche de Chimie Paris, Paris 75005, France.
E-mail addresses: lingjun@zju.edu.cn (J. Ling), min-hui.li@chimieparistech.psl.eu (M.-H. Li).

https://doi.org/10.1016/j.cclet.2019.12.026
1001-8417/

sensitive to oxidation stimuli. Since reactive oxygen species (ROS) and redox reactions are widely present in human body, oxidation-sensitive nanoparticles have been frequently reported as smart drug carriers [24–26]. In a previous work, we synthesized a thioether-bearing polypeptoid, poly(*N*-3-(methylthio)propyl glycine) (PMeSPG), and prepared polymersomes from PMeSPG-*b*-PSar block copolymers [27]. As the hydrophobic thioethers can be oxidized into hydrophilic sulfoxides, the obtained polymersomes showed oxidation-responsive bursting in the presence of hydrogen peroxide (H_2O_2). However, the H_2O_2 used as external stimulus in the study had much higher concentration than the micromolar H_2O_2 level *in vivo*, which limited its realistic use. The production of H_2O_2 *in-situ* in the target site by oxidant-generating enzymes and corresponding substrates is considered to be a more practical way [28]. In this work, we report on polymersomes made of poly(ethylene glycol)-*b*-poly(*N*-3-(methylthio)propyl glycine) (PEG-*b*-PMeSPG), which can encapsulate glucose oxidase (GOx), an enzyme which can oxidize glucose and generate H_2O_2. We demonstrate the disruption of polymersomes after the incubation with D-glucose. PEG-*b*-PMeSPG block copolymers with different PMeSPG chain lengths were synthesized by ring-opening polymerization (ROP) of *N*-3-(methylthio)propyl glycine *N*-thiocarboxyanhydride (MeSPG-NTA) initiated by amino-terminated PEG [29,30]. Their self-assembly was performed by nanoprecipitation and double emulsion method. The influence of the organic cosolvent in nanoprecipitation on the nanostructures was discussed in detail. PEG-*b*-PMeSPG polymersomes loaded with GOx were prepared by double emulsion method followed by extrusion treatment. Finally, the oxidation-responsive disruption of polymersomes was achieved after the incubation with D-glucose with the *in-situ* production of H_2O_2.

The monomer MeSPG-NTA was prepared as described in our previous work [27]. The synthesis of PEG-*b*-PMeSPG was performed through the ROP of MeSPG-NTA using amino-terminated PEG with molecular weight (MW) of 2000 Da (PEG_{45}-NH_2) as a macromolecular initiator (Fig. 1). With various feeding ratios of monomers to initiator, three amphiphilic block copolymers PEG-*b*-PMeSPG, EM1 (PEG_{45}-*b*-$PMeSPG_{17}$), EM2 (PEG_{45}-*b*-$PMeSPG_{40}$) and EM3 (PEG_{45}-*b*-$PMeSPG_{71}$), were obtained with different MWs and hydrophilic/hydrophobic ratios (Table 1). The MW distributions ($Đ$) of the copolymers were controlled within 1.2. The compositions of blocks were determined by the characteristic signals in ^{1}H NMR spectrum (Fig. S1A for spectrum of EM3 and calculation in Supporting information). The SEC traces (Fig. S1B in Supporting information) exhibited monomodal MW distributions for all three copolymers, which shifted from right to left as the degree of polymerization (DP) of PMeSPG block increased. These results suggested good controllability of the polymerization.

As the most common approach for self-assembly of block copolymers, nanoprecipitation was first employed to prepare PEG-*b*-PMeSPG nanoparticles dispersed in water. *N,N*-dimethylformamide (DMF) and tetrahydrofuran (THF) were chosen as the organic cosolvents, respectively, to dissolve the copolymers at a concentration of 5 g/L. Then water (2 mL) was added to the solution (1 mL) at the rate of 0.2 mL/h, driving the hydrophobic blocks to assemble together to avoid their contact with water and form finally nanostructures. The organic solvent was removed at the end by dialysis against water, leading to aqueous dispersions of polymer nanoparticles. The morphologies were analyzed by cryogenic electronic microscopy (Cryo-EM).

We discuss first the polymer nanoparticles formed using DMF as the nonselective cosolvent. As revealed by Cryo-EM images (Fig. 2A and Figs. S2A–C in Supporting information), nanospheres with diameters around 20 – 90 nm were obtained from EM1 with the hydrophilic ratio of 45%. Along with the spheres, a few unilamellar vesicles were also observed (Figs. S2B and C) with diameters

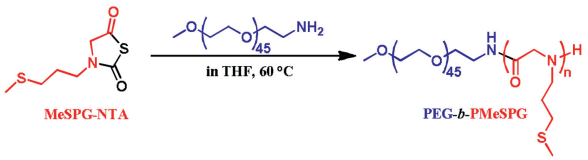

Fig. 1. Synthesis of PEG-*b*-PMeSPG by ROP of MeSPG-NTA.

around 50 – 130 nm, and membrane thickness around 9 nm. EM2 with hydrophilic ratio of 26% formed spherical and worm-like micelles, whose diameters were around 18 – 21 nm (Fig. 2C and Figs. S2D-F in Supporting information). EM3 with hydrophilic ratio of 16% and the largest MW (12,300 Da) in these three copolymers self-assembled into polymersomes with broad size distribution (diameters = 50 – 550 nm) and membrane thickness around 12 – 14 nm (Figs. 2E and S2G–I in Supporting information). Simultaneously, lamellae were observed together with vesicles, and many of them were in disk-like shapes (Figs. S2H and I in Supporting information). Lamellae also had a diversity of size in the range of 250 – 2000 nm. Their thickness could be measured in the folded region of lamellae, which was found to be around 12 nm, similar to that of the vesicular membrane. As a widely accepted mechanism, vesicles were formed by the closure of open lamellae, when the edge energy of the lamellae meets with the bending energy for closed vesicles [31]. Intermediate structures are often observed in the self-assembly of polymers as "frozen" metastable states, because of the relatively high molecular weights of polymers. Therefore, the coexistence of folded lamellae, incomplete vesicles and closed vesicles in Fig. S2I could be considered as an evidence for the above mechanism of vesicle formation.

When THF was used as the organic cosolvent instead of DMF in nanoprecipitation, the morphologies of the nanostructures self-assembled from the three copolymers were totally different. EM1 formed many long fibers and ribbons (Figs. 2B and S3A–C in Supporting information). Fibers had the width around 5 – 6 nm, ribbons around 21 – 23 nm. EM2 formed lamellae with irregular and fragmented shapes (Fig. 2D and Figs. S3D–F in Supporting information), of which the membrane thickness was measured to be around 10 – 11 nm. For EM3 (Fig. 2F and Figs. S3G–I in Supporting information), lamellae with large area (over 2 μm) were observed predominantly, with the membrane thickness around 14 – 16 nm. The self-assembled nanostructures and their sizes discussed above were summarized in Table S1 (Supporting information).

The overall morphology of nanoparticles self-assembled by amphiphiles in water depends firstly on their packing parameter p [11,32]. p is a geometric parameter, $p = V/a_0l$, where V is the volume of the hydrophobic part, l its length, and a_0 the equilibrium area at the core/corona interface. As p increases from below 1/3 to equaling to 1, the preferred morphology changes from sphere, to cylinder, vesicle, and finally flat lamella. In the case of amphiphilic block copolymers, p is strongly related to the ratio of hydrophilic/hydrophobic blocks. For the copolymers PEG_{45}-*b*-$PMeSPG_n$, p increases when DP of the hydrophobic block PMeSPG increases. Indeed, the copolymers EM1, EM2 and EM3 showed a typical morphological change of "spheres – cylinders – vesicles" with DMF as the organic cosolvent.

From the same copolymer, different morphologies of self-assemblies were obtained by choosing different organic solvents. It indicated the effect of solvent on copolymer self-assembly. This observation can be explained by the different polymer – solvent interactions. The solubility parameter δ is an important parameter to characterize the polymer – solvent interactions. δ is contributed by three components, as presented by Eq. 1, where δ_d represents the dispersion force, δ_p the polar interaction, and δ_h the hydrogen

Table 1
Syntheses of PEG-b-PMeSPG copolymers.

Copolymers	[M]/[I]	Yield	DP_{MeSPG}/DP_{EG}[a]	$f_{PEG,wt}$[a]	$M_{n,\ NMR}$[a]	$M_{n,\ SEC}$[b]	$Đ$[b]
EM1	14	91.1%	17/45	45%	4500	3600	1.14
EM2	39	83.2%	40/45	26%	7800	4900	1.19
EM3	82	82.5%	71/45	16%	12300	7700	1.15

[a] DP, MW and PEG weight ratio ($f_{PEG,wt}$) were calculated from the integrals of characteristic signals in ^{1}H NMR spectra (Supporting information).
[b] Determined by SEC calibrated with PEG standards (eluent: 0.01 mol/L LiBr/DMF at the rate of 1 mL/min).

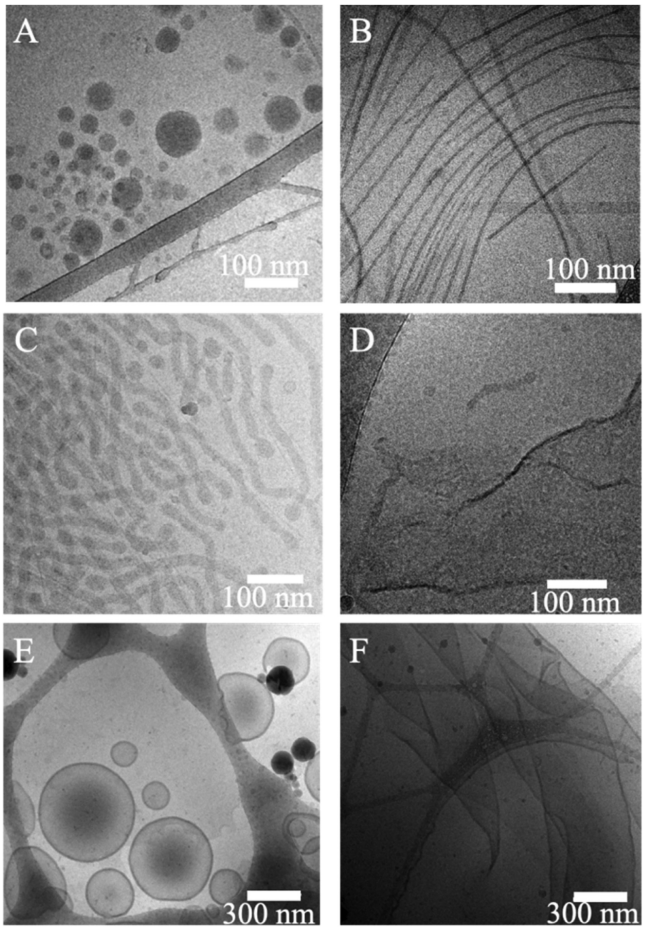

Fig. 2. Cryo-EM images of self-assemblies obtained by nanoprecipitation from EM1 (A, B), EM2 (C, D) and EM3 (E, F). DMF (A, C and E) and THF (B, D and F) were chosen as the organic cosolvents in nanoprecipitation experiments, respectively.

bonding. The miscibility between polymer and solvent can be predicted by the solubility parameter difference $\Delta\delta_{P\text{-}S}$ [33,34], as calculated by Eq. 2.

$$\delta^2 = {\delta_d}^2 + {\delta_p}^2 + {\delta_h}^2 \quad (1)$$

$$\Delta\delta_{P-S} = ((\delta_{d,P} - \delta_{d,S})^2 + (\delta_{p,P} - \delta_{p,S})^2 + (\delta_{h,P} - \delta_{h,S})^2)^{1/2} \quad (2)$$

The solubility parameters and their components of the DMF, THF, PEG and PMeSPG were listed in Table S2 (Supporting information). Among them the values of DMF and THF were reported by Hansen *et al.* [33], while the values of PEG and PMeSPG were calculated by a group contribution method (Hoy's method) [34–36]. By putting these values into Eq. 2, we were able to obtain the differences between the solubility parameters of polymer and solvent $\Delta\delta_{P\text{-}S}$. Generally, a smaller $\Delta\delta_{P\text{-}S}$ indicates a better miscibility between polymer and solvent [34]. For PEG, $\Delta\delta_{PEG\text{-}DMF}$ = 4.46 $MPa^{1/2}$ and $\Delta\delta_{PEG\text{-}THF}$ = 4.54 $MPa^{1/2}$, while for PMeSPG, $\Delta\delta_{PMePG\text{-}DMF}$ = 6.89 $MPa^{1/2}$ and $\Delta\delta_{PMeSPG\text{-}THF}$ = 7.43 $MPa^{1/2}$. The relatively low values of $\Delta\delta_{PEG\text{-}DMF}$ and $\Delta\delta_{PEG\text{-}THF}$ suggest DMF and THF are both good solvents for PEG with nearly equivalent miscibility. By comparing $\Delta\delta_{PMePG\text{-}DMF}$ and $\Delta\delta_{PMeSPG\text{-}THF}$, it can be concluded that the miscibility between PMeSPG and DMF is better than that between PMeSPG and THF. During the nanoprecipitation procedure, when water (a poor solvent for PMeSPG) was added into the system, the hydrophobic blocks self-assembled together to avoid their exposure to water. In the hydrophobic regions, organic solvents still coexisted during the water addition, and more solvent molecules remained in the copolymer aggregates in the case of DMF/water system than in the case of THF/water system. This difference in solvent content may further result in different self-assembled morphologies. Take EM3 for example, when water was added into the EM3/DMF solution, some DMF molecules stayed in the bilayer membranes formed by copolymers, and played the role of plasticizers. Consequently, the membrane was flexible and had low bending modulus, which could close like a pulled bag to form vesicles. However, when the nanoprecipitation of EM3 was proceeded in EM3/THF solution, the self-assembled bilayer membranes involved fewer solvent molecules than in EM3/DMF, and the relatively low flexibility of the membrane did not allow the formation of closed vesicles. (Figs. 2E and F)

The solubility behavior of copolymers in self-assembly experiments was in accordance with the calculated results. When the PEG-*b*-PMeSPG copolymers were dissolved in organic cosolvents for nanoprecipitation, we did find that all the copolymers dissolved easily in DMF, while much longer time was taken for the copolymers to be dissolved in THF, especially for EM3, heating was necessary for dissolution. Similar cases were reported on the solubility of other polypeptoids. PSar, also called as poly(*N*-methyl glycine), was soluble in DMF, but insoluble in THF [2]. Schlaad *et al.* also found that polypeptoids including poly(*N*-allyl glycine) and poly(*N*-3-(glycerolthio)propyl glycine) had obviously poorer solubility in THF than in DMF [37]. Especially poly(*N*-3-(glycerolthio) propyl glycine), which was synthesized from thiol-ene coupling between poly(*N*-allyl glycine) and 1-thiolglycerol, had thioether-containing sidechains like PMeSPG, and was hardly dissolved in THF but well dissolved in DMF. In general, there was no polypeptoid reported, which exhibited better solubility in THF than in DMF.

Besides nanoprecipitation, double emulsion method is another interesting approach to prepare polymersomes with the advantage of high yield, where the bilayer vesicles were formed from water-in-oil-in-water (W/O/W) double emulsions [38,39]. In the previous work, we used this method successfully to prepare polypeptoid vesicles [27]. Here we prepared EM2 polymersomes by double emulsion method (experimental details in Supporting information). Giant vesicles were first obtained with the diameter of $2-10\ \mu m$, as observed by confocal laser scanning microscopy (CLSM), where the vesicles were visualized by Nile Red loaded in the membrane (Fig. 3A). Extrusion treatment was employed on the giant vesicle dispersion [40], using a mini lipid extruder (Avanti® Mini-Extruder, Avanti Polar Lipids, USA) with 200 nm polycarbonate membranes, which yielded nano-polymersomes (Fig. 3C). The

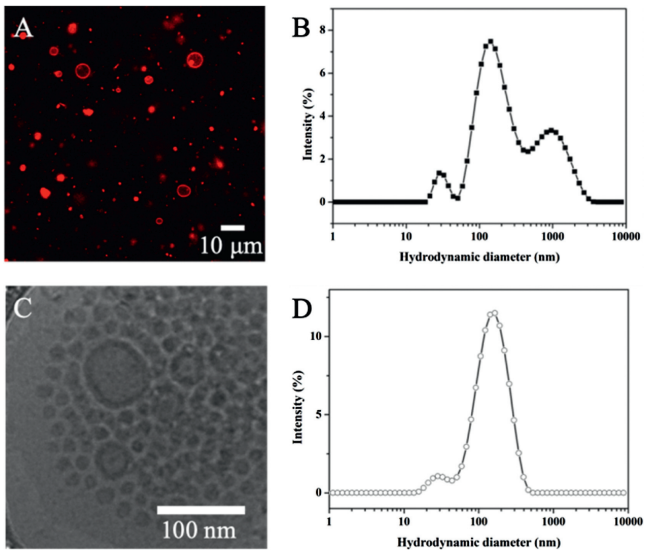

Fig. 3. (A) CLSM image and (B) DLS distribution curve of giant polymersomes EM2 from double emulsion; (C) Cryo-EM image and (D) DLS distribution curve of the EM2 self-assemblies obtained using double emulsion method followed by extrusion treatment. In CLSM image, Nile Red was loaded in the membrane for visualization.

change in sizes and distributions were analyzed by dynamic light scattering (DLS), which revealed a multi-peak distribution curve (Fig. 3B) transforming into a nearly monomodal curve, with a main peak around 160 nm (Fig. 3D).

Since the pendant thioether groups on hydrophobic blocks of PEG-*b*-PMeSPG can be oxidized into hydrophilic sulfoxide groups, the PEG-*b*-PMeSPG polymersomes have the potential to be disrupted under the action of oxidation stimuli. The GOx-encapsulated polymersomes were then prepared by adding GOx/PBS to EM2/chloroform solution when performing the double emulsion (See Supporting information for detailed procedure). After extrusion treatment, nano-polymersomes were obtained with the concentration of 0.5 g/L for both polymer and GOx. D-Glucose (25 mmol/L) was then introduced to the dispersion of GOx-loaded EM2 nano-polymersomes. DLS was performed to monitor the change in the polymersomes in the following 240 min at 37 °C. The loaded glycoprotein enzyme GOx is a dimer consisting of 2 equal subunits with a molecular mass of 80 kDa each. Each subunit contains one flavin adenine dinucleotide (FAD, a cofactor) moiety and one iron. FAD works as the initial electron acceptor in redox reaction and can be reduced into $FADH_2$. During the oxidation of D-glucose into gluconolactone by the catalysis of GOx, H_2O_2 is generated in presence of dissolved oxygen. It is H_2O_2 that transfers the hydrophobic thioether groups of PMeSPG into hydrophilic sulfoxides [27], eventually inducing the destabilization of polymersomes (Fig. 4A). In DLS, the count rates represented the scattering intensity and indicated the size and/or concentration of particles. As revealed in Fig. 4B, the count rates decreased mildly in the first 60 min, afterwards from 60 min to 140 min, the count rates dropped abruptly from around 900 kcps to 200 kcps. The count rates decreased slightly after 140 min, and fell to 110 kcps at 240 min. The size and size distribution were also assessed during the incubation with D-glucose. As shown in Fig. 4C, the hydrodynamic diameter of the polymersomes kept stable at around 145 nm in the first 60 min, and then decreased significantly from 145 nm to around 70 nm during 80–160 min. The diameter kept around 70 nm steadily until 240 min. Meanwhile, the

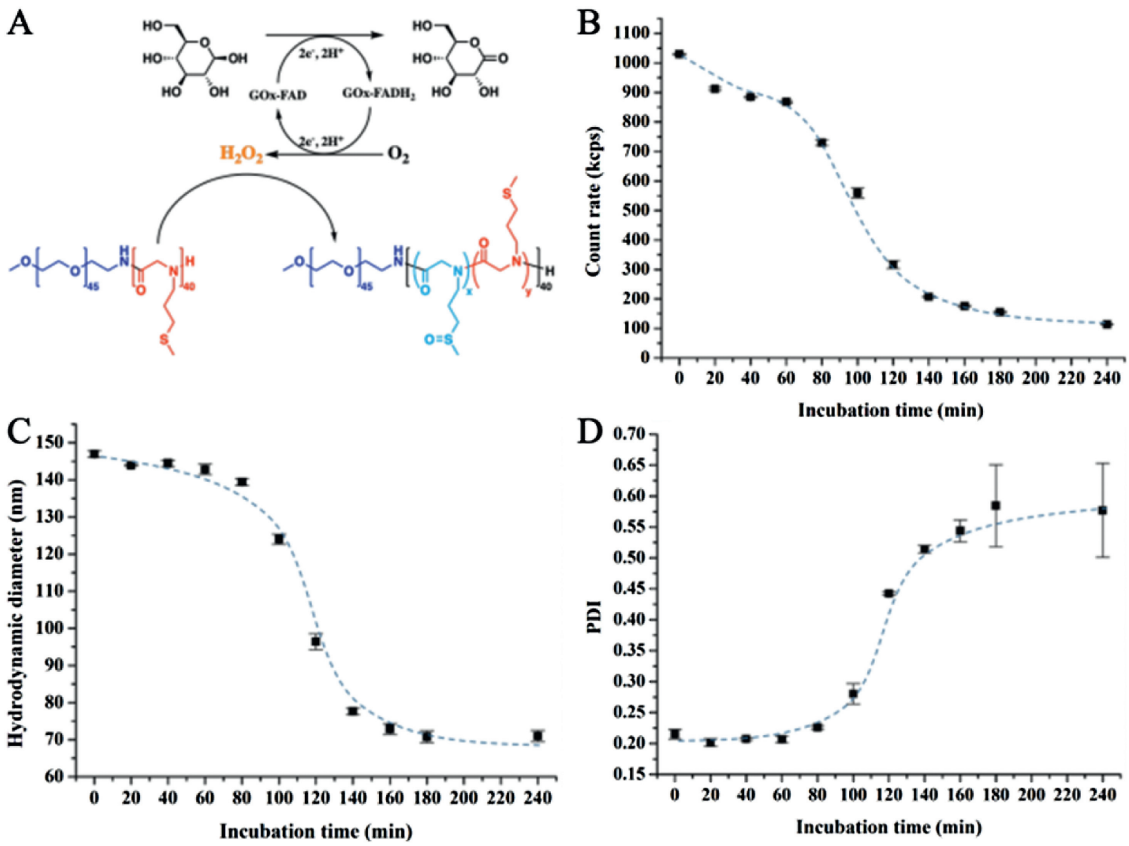

Fig. 4. (A) Schematic illustration of the GOx-catalyzed conversion of D-glucose into gluconolactone with production of H_2O_2, transferring the pendant hydrophobic thioether groups of EM2 into hydrophilic sulfoxides; the evolution of (B) count rates, (C) hydrodynamic diameter (Z-average diameter) and (D) size distribution (PDI) of GO_x-loaded EM2 polymersomes (0.5 mg copolymer, 0.5 mg GO_x in 1 mL PBS) as a function of time of incubation with 25 mmol/L glucose at 37 °C.

polydispersity index (PDI, Fig. 4D) kept stable at around 0.2 in the first 60 min, and then started to increase, from 0.2 to around 0.5 from 80 min to 160 min. The PDI reached to 0.58 at 240 min. Note that from the time $t = 180$ min, the PDI value fluctuated intensely. As visualized by Cryo-EM (Fig. S4 in Supporting information), micelles and aggregates with various shapes and sizes below 100 nm took the majority in the sample after the incubation.

The evolution of GOx-loaded polymersomes observed in DLS as a function of the incubation time with D-glucose observed could be explained as follows. The glass transition temperature (T_g) of PMeSPG was dertermined by differential scanning calorimetry (DSC) analyses ($PMeSPG_{45}$ and $PMeSPG_{85}$, Fig. S5 in Supporting information). A rather low T_g around 20–30 °C was measured, which was below both the body temperature and the temperature of incubation here. Therefore, hydrophobic blocks PMeSPG in the vesicle membrane had good mobility at 37 °C, which might favor the diffusion of glucose across the membrane and got involved in the oxidation process to eventually induce polymersome disruption [41]. When the vesicles were dissembled and GO_x was released, the free enzymes had lower concentration than that of the encapsulated enzymes [41], therefore the redox reaction slowed down. Finally, the system contained smaller but more stable micelles composed of incompletely oxidized copolymers.

In conclusion, we present here the synthesis and self-assembly of the amphiphilic block copolymers PEG-*b*-PMeSPG, with three different chain lengths of the hydrophobic block PMeSPG. Nanoprecipitation with DMF and THF as the organic cosolvents was used first to prepare the polypeptoid nanoparticles. Various morphologies such as spheres, fibers, lamellae and vesicles were observed for different copolymers depending on the hydrophilic/hydrophobic ratio and the cosolvent. Double emulsion method followed by extrusion treatment was employed then to prepare EM2 polymersomes and GOx-loaded EM2 polymersomes. GOx-loaded polymersomes could be disrupted under the action of oxidants generated *in-situ* in the presence of D-glucose. These polymersomes may find applications in drug delivery and can also be used for the design of micro/nano-reactors, biosensors and biodetectors.

Declaration of competing interest

The authors declare that they have no known competing financial interests or personal relationships that could have appeared to influence the work reported in this paper.

Acknowledgments

We acknowledge the French National Research Agency (No. ANR-16-CE29-0028), the National Natural Science Foundation of China (No. 21674091) and the Joint Foundation of Shaanxi Province Natural Science Basic Research Program and Shaanxi Coal Chemical Group Co., Ltd. (No. 2019JLM-46) for financial support. Y. Deng thanks the China Scholarship Council for funding his Ph.D. scholarship in France. The authors would like to thank the PICT Ibisa for providing access to the cryo electron microscopy facility at Orsay.

Appendix A. Supplementary data

Supplementary material related to this article can be found, in the online version, at doi:https://doi.org/10.1016/j.cclet.2019.12.026.

References

[1] B.A. Chan, S. Xuan, A. Li, et al., Biopolymers 109 (2018) e23070.
[2] A. Birke, J. Ling, M. Barz, Prog. Polym. Sci. 81 (2018) 163–208.
[3] N. Gangloff, J. Ulbricht, T. Lorson, H. Schlaad, R. Luxenhofer, Chem. Rev. 116 (2016) 1753–1802.
[4] S.H. Lahasky, X. Hu, D. Zhang, ACS Macro Lett. 1 (2012) 580–584.
[5] C. Secker, S.M. Brosnan, R. Luxenhofer, H. Schlaad, Macromol. Biosci. 15 (2015) 881–891.
[6] J. Ulbricht, R. Jordan, R. Luxenhofer, Biomaterials 35 (2014) 4848–4861.
[7] J. Sun, X. Jiang, A. Siegmund, et al., Macromolecules 49 (2016) 3083–3090.
[8] C. Fetsch, S. Flecks, D. Gieseler, et al., Macromol. Chem. Phys. 216 (2015) 547–560.
[9] G.L. Sternhagen, S. Gupta, Y. Zhang, et al., J. Am. Chem. Soc. 140 (2018) 4100–4109.
[10] X. Fu, J. Tian, Z. Li, J. Sun, Z. Li, Biopolymers 110 (2019) e23243.
[11] A. Blanazs, S.P. Armes, A.J. Ryan, Macromol. Rapid Commun. 30 (2009) 267–277.
[12] J. Sun, X. Jiang, R. Lund, et al., Proc. Natl. Acad. Sci. U. S. A. 113 (2016) 3954–3959.
[13] C. Fetsch, J. Gaitzsch, L. Messager, G. Battaglia, R. Luxenhofer, Sci. Rep. 6 (2016) 33491.
[14] X. Jiang, R.K. Spencer, J. Sun, et al., J. Phys. Chem. B 123 (2019) 1195–1205.
[15] S. Xuan, C.U. Lee, C. Chen, et al., Chem. Mater. 28 (2016) 727–737.
[16] L. Zhu, J.M. Simpson, X. Xu, et al., ACS Appl. Mater. Interfaces 9 (2017) 23476–23486.
[17] A. Li, D. Zhang, Biomacromolecules 17 (2016) 852–861.
[18] X. Tao, H. Chen, S. Trépout, et al., Chem. Commun. (Camb.) 55 (2019) 13530–13533.
[19] M.H. Li, P. Keller, Soft Matter 5 (2009) 927–937.
[20] W. Chen, J. Du, Sci. Rep. 3 (2013) 2162.
[21] X. Hu, Y. Zhang, Z. Xie, et al., Biomacromolecules 18 (2017) 649–673.
[22] Y. Deng, J. Ling, M.H. Li, Nanoscale 10 (2018) 6781–6800.
[23] B. Yang, J. Du, Sci. China Chem. 63 (2020) 272–281.
[24] Z. Deng, J. Hu, S. Liu, Macromol. Rapid Commun. 38 (2017) e1600685.
[25] S.H. Lee, M.K. Gupta, J.B. Bang, H. Bae, H.J. Sung, Adv. Healthc. Mater. 2 (2013) 908–915.
[26] C.C. Song, F.S. Du, Z.C. Li, J. Mater. Chem. B Mater. Biol. Med. 2 (2014) 3413–3426.
[27] Y. Deng, H. Chen, X. Tao, et al., Biomacromolecules 20 (2019) 3435–3444.
[28] M. Ikeda, T. Tanida, T. Yoshii, et al., Nat. Chem. 6 (2014) 511–518.
[29] B. Zheng, X. Tao, J. Ling, Acta Polymer. Sin. (2018) 72–79.
[30] X. Tao, M.H. Li, J. Ling, Eur. Polym. J. 109 (2018) 26–42.
[31] M. Antonietti, S. Forster, Adv. Mater. 15 (2003) 1323–1333.
[32] A.H. Groeschel, A. Walther, Angew. Chem. Int. Ed. 56 (2017) 10992–10994.
[33] C.M. Hansen, Hansen Solubility Parameters: A User's Handbook, 2nd ed., CRC Press, 2007.
[34] D.W. van Krevelen, K. te Nijenhuis, Properties of Polymers: Their Correlation With Chemical Structure; Their Numerical Estimation and Prediction From Additive Group Contributions, Elsevier Science, 2009.
[35] C. Özdemir, A. Güner, Eur. Polym. J. 43 (2007) 3068–3093.
[36] K.L. Hoy, Tables of solubility parameters, Union Carbide Solvents and Coatings Materials Division, 1984.
[37] J.W. Robinson, H. Schlaad, Chem. Commun. (Camb.) 48 (2012) 7835–7837.
[38] H.C. Shum, Y.J. Zhao, S.H. Kim, D.A. Weitz, Angew. Chem. Int. Ed. 50 (2011) 1648–1651.
[39] J. Bae, T.P. Russell, R.C. Hayward, Angew. Chem. Int. Ed. 53 (2014) 8240–8245.
[40] H.B. Zhang, W.G. Cui, X.M. Qu, et al., Proc. Natl. Acad. Sci. U. S. A. 116 (2019) 7744–7749.
[41] A. Napoli, M.J. Boerakker, N. Tirelli, et al., Langmuir 20 (2004) 3487–3491.